Original Article

Institution of MECHANICAL ENGINEERS
Journal of MECHANICAL ENGINEERING SCIENCE

Proc IMechE Part C:
J Mechanical Engineering Science
227(11) 2531–2548

DOI: 10.1177/0954406213475947
pic.sagepub.com
SAGE

Design of a network of robotic Lagrangian sensors for shallow water environments with case studies for multiple applications

Carlos Oroza[1], Andrew Tinka[2], Paul K Wright[3] and Alexandre M Bayen[4]

Abstract

This article describes the design methodology for a network of robotic Lagrangian floating sensors designed to perform real-time monitoring of water flow, environmental parameters, and bathymetry of shallow water environments (bays, estuarine, and riverine environments). Unlike previous Lagrangian sensors which passively monitor water velocity, the sensors described in this article can actively control their trajectory on the surface of the water and are capable of inter-sensor communication. The addition of these functionalities enables Lagrangian sensing in obstacle-encumbered environments, such as rivers. The Ishikawa cause and effect design framework is used to ensure that the final system synthesizes the diverse operational and functional needs of multiple end-user groups to arrive at a broadly applicable system design. A summary of potential applications for the system is given including completed projects performed on behalf of the Department of Homeland Security, Office of Naval Research, and the California Bay-Delta Authority.

Keywords

Robotics, mobile sensors, Ishikawa diagram, hydrodynamics

Date received: 11 June 2012; accepted: 11 December 2012

Introduction

A Lagrangian sensor is an instrument used in the field of oceanography and hydrodynamics to monitor the currents and other physical properties of large-scale hydraulic systems. The instrument measures the water velocity by moving within the medium, along a trajectory of the flow (as opposed to an 'Eulerian' sensor which measures the properties of the medium from a fixed location). It measures other physical properties, such as temperature, turbidity, and dissolved oxygen, with a variety of onboard sensors. Lagrangian sensors have seen extensive use in the oceanographic community since 1955.[1] In the field, they are referred to as 'drifters'. Early drifters used acoustic communication to transmit data to researchers.[2] Their capabilities expanded in 1978 with the introduction of the Argos satellite service, which enabled remote communication of sensor data and location.[3] Examples of Argos-enabled units include the Costal Dynamics Experiment Drifter,[4] and the Low Cost Tropical Drifter.[5] In the oceanographic community, these sensors are usually 'passive', meaning they have no actuation capabilities.

The design of oceanographic drifters generally consists of a buoyant spherical or cylindrical housing for the sensors and communications equipment which is tethered to a drogue. The drogue extends into the water and is designed to capture the current by presenting a large, symmetric drag profile to oncoming flow. For example, the Low Cost Tropical Drifter's sensor housing is a PVC tube which is 11.4 cm diameter and 2.9 m long. It is designed to be positively buoyant such that 0.4 m of the cylinder are above the surface of the water. The drogue is attached by a 7.5 m nylon tether which is 1.6 cm in diameter. The drogue itself is a perforated cylindrical tube which is 10 m long and 50 cm in diameter. Similarly, the TRISTAR drifter consists of a 48-cm fiberglass

[1]Department of Civil and Environmental Engineering, University of California, Berkeley, CA, USA
[2]Department of Electrical Engineering and Computer Sciences, University of California, Berkeley, CA, USA
[3]Department of Mechanical Engineering, University of California, Berkeley, CA, USA
[4]Department of Electrical Engineering and Computer Sciences, University of California, Berkeley, CA, USA

Corresponding author:
Andrew Tinka, Department of Electrical Engineering and Computer Sciences, Mail Box #10, 2594 Sutardja Dai Hall, Berkeley, CA 94720-1758, USA.
Email: tinka@berkeley.edu

sphere tethered to a 557 cm × 544 cm symmetric drogue.

A logical extension of the oceanographic research in Lagrangian sensing is to develop sensors for near-shore environments such as rivers and bays. It is important to instrument such environments because the majority of renewable freshwater available for human use flows through rivers.[6] Lagrangian sensors can be used in this context to better monitor the flow of freshwater and the transport of constituents therein. Specific examples include assessing vulnerabilities to contaminate spills or infrastructure failure in critical water-resource regions, planning reservoir release and gate control policies to affect the intrusion of salt water, and monitoring the effect of heavy agriculture use on freshwater supplies.

However, simply scaling down the oceanographic design paradigm will not work for Lagrangian sensors operating in constricted domains. In such environments, the possible locations of the sensor represent more space relative to the boundaries of the environment and sensors can easily become entangled on the shore. Also, because rivers are obstacle-encumbered and contain many branches, there are situations in which the sensor's motion must be actively controlled, rendering passive sensors less useful for monitoring missions. Finally, in rivers, sensors move through the experimental domain faster, requiring more frequent deployments and retrievals. Thus, a new sensor must be designed that retains a suitable form factor for Lagrangian sensing, but adds capabilities such as active control and inter-vehicle communication.

Fortunately, recent developments in sensor networks for aquatic sensing has made operations in constricted environments feasible. Examples include the AMOUR project at MIT,[7] the NEPTUS Autonomous Underwater Vehicle (AUV) at LSTS in Portugal,[8] submersible pneumatic drogues built at UCSD,[9] the Slocum underwater drifters at MBARI,[10] and the Smart Bay sensor network in Galway Bay.[11] In many cases, these projects have added the communication and actuation capabilities necessary for operations in constricted environments. However, many of these AUVs, such as the submarines used in LSTS, are not suited for Lagrangian sensing in rivers specifically. The overall size and shape of a submarine is not appropriate for Lagrangian sensing since it does not present a symmetric drag profile to the flow and the deployments require specialized equipment. The authors are unaware of any previously existing active Lagrangian sensor network for use in shallow water environments such as rivers and bays.

This article details the design for the physical sensors in such a network. The use of a design methodology adapted from the Ishikawa 'cause and effect' framework (discussed in detail below) has enabled the creation of an electro-mechanical system which balances the diverse needs of a wide range of end-user groups. This article presents an overview of the *Floating Sensor Network* system, a discussion of the design methodology used for the physical sensors, and a detailed explanation of how each component of the system evolved from the methodology. The article concludes with three case studies in which the design decisions were validated in real-world tests.

System design overview

The UC Berkeley *Floating Sensor Network*[12] is a system of robotic Lagrangian sensors designed for use in shallow water environments.[13,14] The system is comprised of the robotic sensors shown in Figure 1 as well as the communication and visualization infrastructure required to transmit and display the data in real time.

Each robotic sensor consists of a cylindrical hull which contains the batteries, communications equipment, GPS, and onboard processors. Onboard sensors for salinity, temperature and depth protrude from the base of the vehicle.

Figure 2 shows a schematic of the full drifter-backend system, which consists of an integrated computational support tool and platform linked to the floating sensors. Data from the sensors can be intercommunicated between vehicles using 802.15.4 radios. Data are also sent back to a central server using the Global System for Mobile Communications (GSM) cell phone data network. The system enables the data from the sensors to be assimilated and visualized in real time, giving the end user live access to the sensor data. It also assists field operations by

Figure 1. *Floating Sensor Network* vehicle design.

providing a constant stream of vehicle diagnostics and position data.

The velocity measurements inferred from GPS can be combined with measurements from a static infrastructure maintained by the US Geological Survey.[14] The computations necessary to take data from the sensors in the field and create an estimate of the entire system is called data assimilation. This is an estimation problem characterized by sparse sensor data. Several techniques can be used to perform data assimilation using these streaming data measurements. For example, the velocity estimates can be assimilated with an ensemble Kalman filter algorithm to generate velocity estimates for the rest of the river system.[14,15] This technique incorporates the sparse sensor data with a model of the hydrodynamic system, such as a two-dimensional shallow water equation, to arrive at an improved state estimate of the system. These estimates are sent back to the processors on the vehicles for path planning.

The vehicle positions, sensors readings, and state estimates from the ensemble Kalman filter algorithm are available online in real time through a visualization tool developed at UC Berkeley called DIVA built on Google mapping technology (see Figure 3).

Design methodology

During the design process of an electro-mechanical system with interrelated system components, it is important to be able to track and prioritize the desired functionalities of the final system. During the prototyping phase of the *Floating Sensor Network*, multiple prototype designs were rejected because they failed to address key system functionalities which were overlooked in the design process. For example, section 'Actuation' describes a prototype actuation system which failed to meet fundamental portability, serviceability, and sensing requirements because they were not sufficiently managed during design. The prototype was developed without a formal design methodology, and its early failure to balance functional requirements underscores the utility of a system to manage the design process.

A general approach to prioritizing and interrelating system components during the design process has been adapted from the Ishikawa 'cause and effect' process.[16,17] In this approach, the desired system functionality is related through a cause and effect or 'fishbone' diagram. The item in the center of the fishbone diagram is the desired outcome for the system, and the branches, or 'causes' leading up to that effect are arranged by priority. In the diagram, components or 'causes' with higher priority are closer to the desired outcome for the system. This approach facilitates prioritization of system functionality during the design process and guides the selection of specific system components. In this manner, once the general system requirements (or 'functional requirements') are enumerated and prioritized, a second fishbone

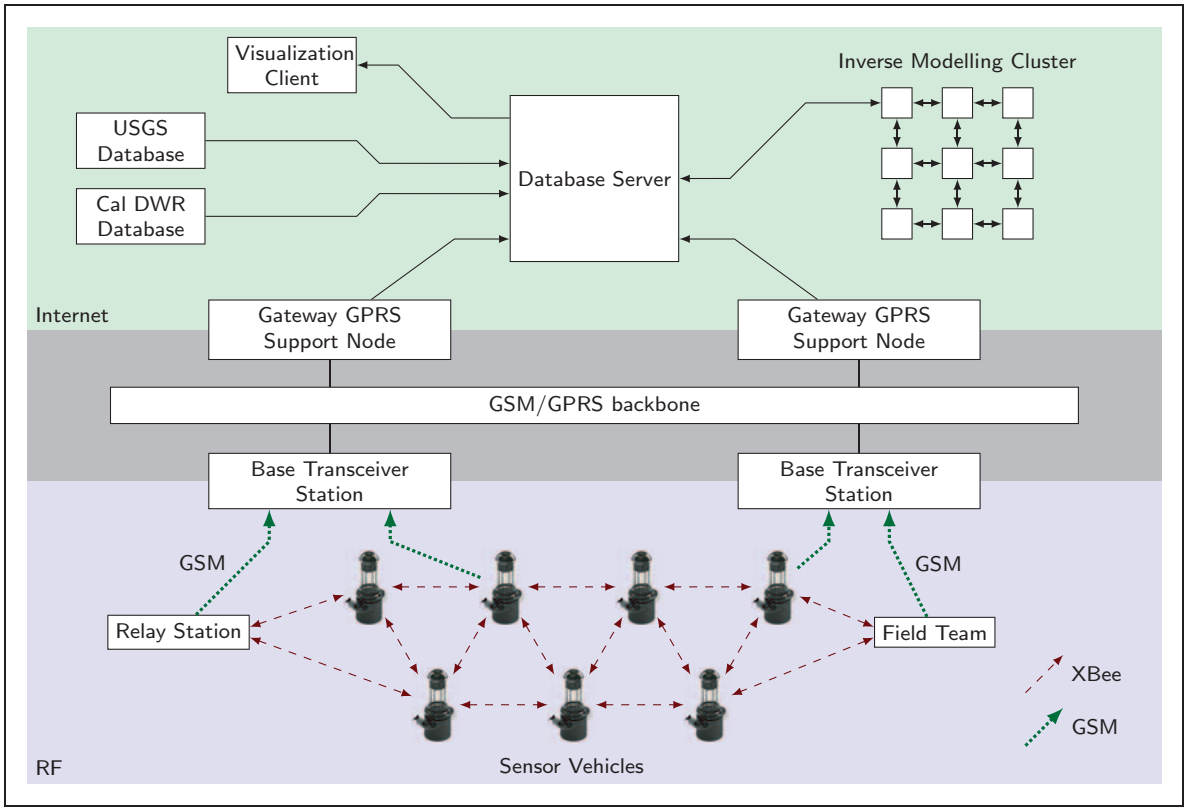

Figure 2. Schematic of the drifter-backend system, including floating sensors and backend computational infrastructure.

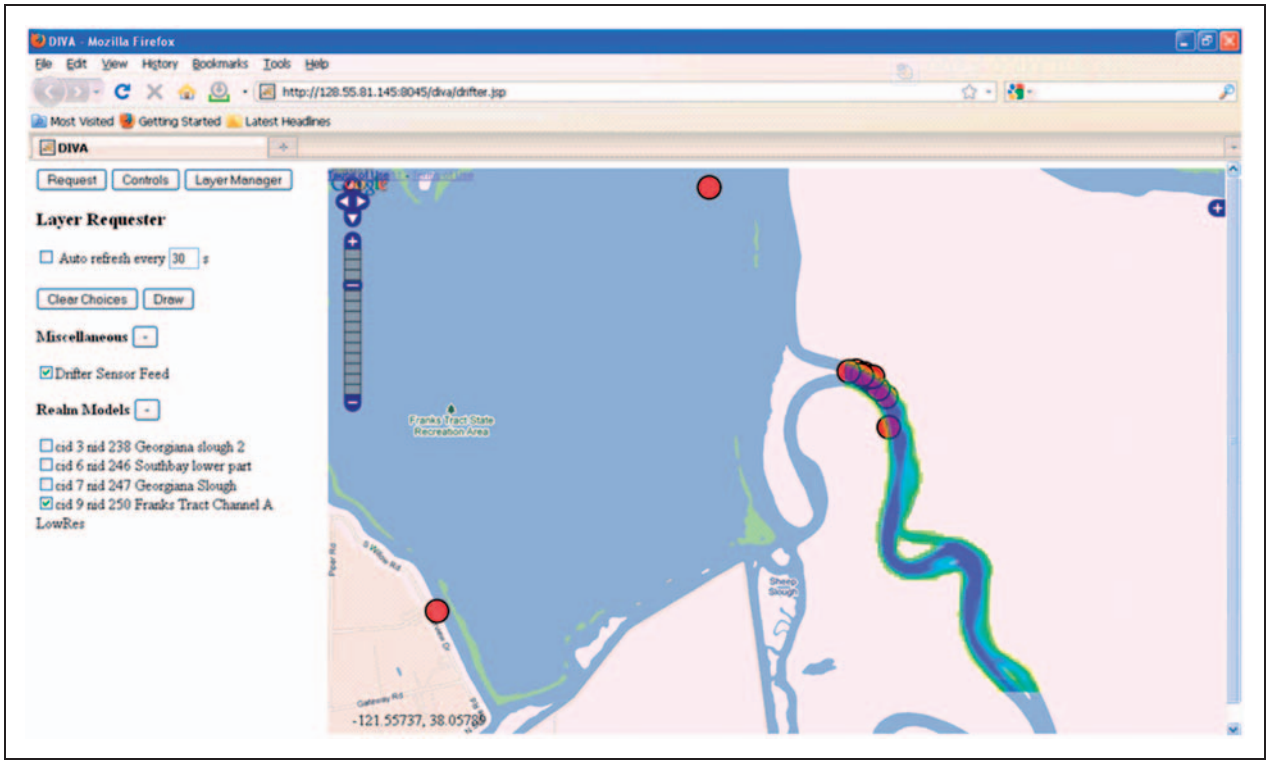

Figure 3. Vehicle position and water velocity computed from the ensemble Kalman filter algorithm running in the background server are available on the web in real time.

diagram can be created with specific 'design parameters' in place of the functional requirements.

The Ishikawa diagram in Figure 4 presents the generic functional requirements of the *Floating Sensor Network*. Figure 5 presents an Ishikawa diagram with the same structure, but with each component replaced with specific 'design parameters'. For example, 'sense location' has been replaced with GPS system, and 'Lagrangian sensor' has been replaced with 'vertical profile, symmetric drag'. The following sections provide a more detailed explanation of how the design parameters for each component on the Ishikawa diagram affect the final system design.

Vehicle design

This section and the next section follow the prioritization order from the Ishikawa diagram. They explain in more detail how the functional requirements from Figure 4 evolved into the specific design parameters listed in Figure 5 during the design process.

Form factor

As indicated by its position in the Ishikawa diagram, the form factor (or overall size and shape of sensor) is one of the most important considerations in the design process since it determines the vehicle's effectiveness as a Lagrangian sensor. Previous studies have indicated that appropriate Lagrangian sensors must maximize their cross-sectional area to flow and should present a roughly symmetric drag profile.[15] Additionally, feedback from researchers and operators in the Office of Naval Research indicated that each sensor should be man portable since the vehicles are usually deployed by a small team from a boat with limited space and/or payload.

To ensure that the vehicle lends itself to Lagrangian sensing, its hull is a vertically oriented cylinder. It is designed to sit low in the water with mass and volume configuration that makes it hydrostatically stable. It must also have a sizable cross-sectional area to ensure that it settles into the local flow as quickly as possible.

Size and weight constraints were enforced during the design process to ensure portability. Each vehicle was not to weigh more than 7 kg, exceed 20 cm in diameter or 50 cm in length.

In order for the system to be broadly applicable for multiple end users, the vehicle must be able to carry a variety of immersed sensors. Therefore, a modular PVC sensor mounting plate was designed into the bottom of the vehicle as shown in Figure 6. It is 12 cm in diameter and 2 cm thick, ensuring ample room exists for a variety of threaded interfaces and o-ring seals.

Finally, to ensure that the vehicles are field serviceable, each functional system is a modular unit which can be easily removed and replaced. As shown in Figure 7, the vehicle consists of the following

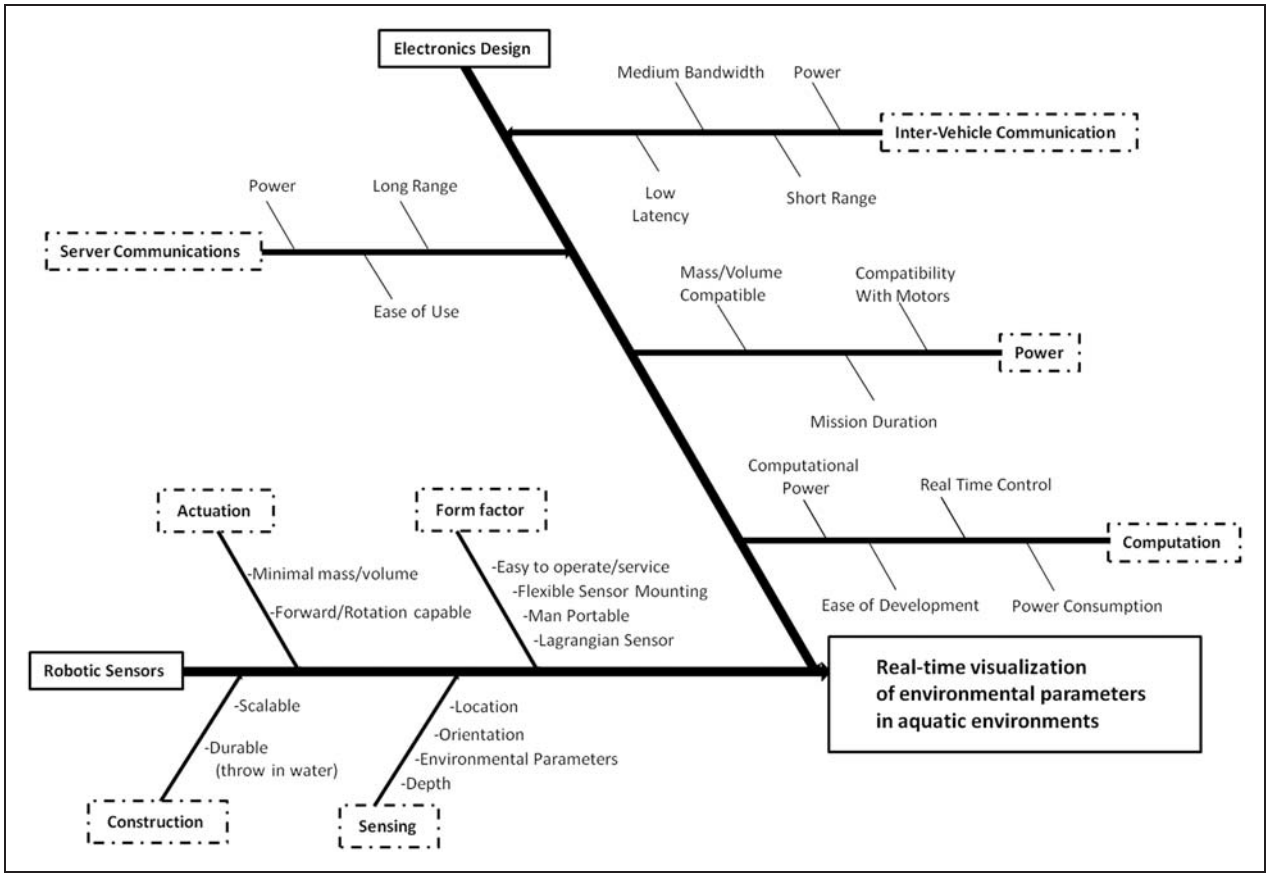

Figure 4. Complete Ishikawa diagram for design process with functional requirements.

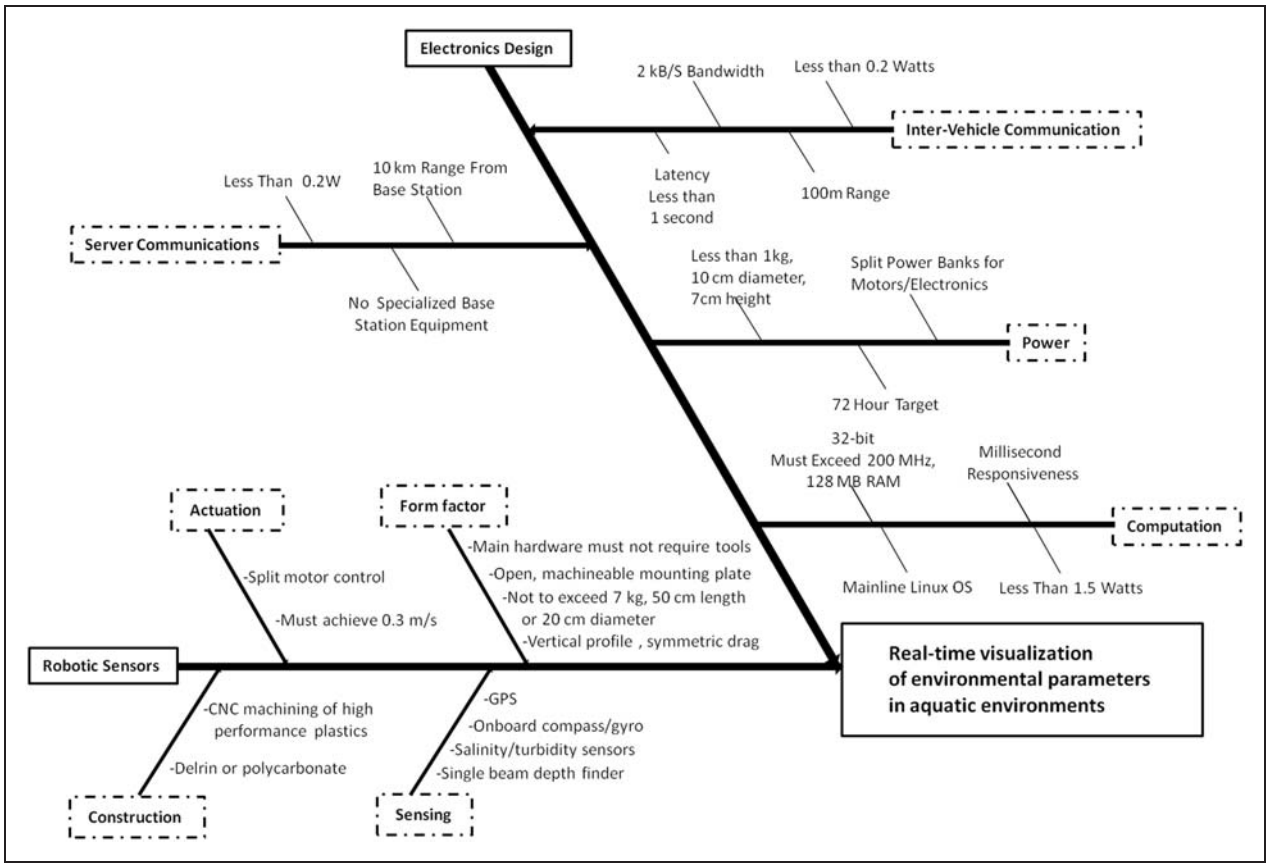

Figure 5. Complete Ishikawa diagram for design process with design parameters.

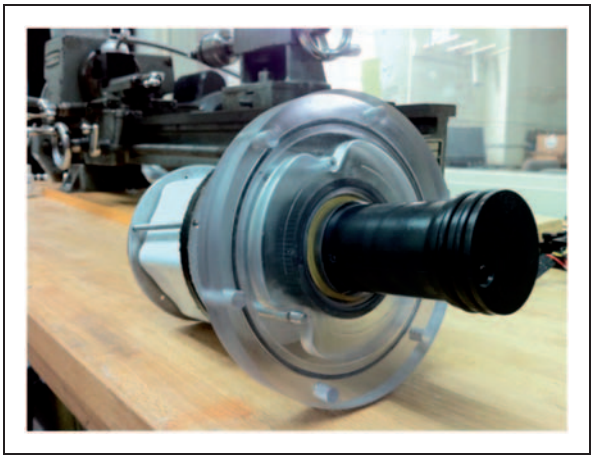

Figure 6. Side view of lower sensor mounting plate with single-beam depth finder installed.

Figure 7. Modular structure of vehicle's internals: (from left to right) Delrin lower hull with removable motor pods, lower electronics assembly with battery and sensors, upper electronics assembly with microprocessors and guidance/location sensors, and clear PVC upper hull.

systems: propulsion pods, power electronics and sensors, and communications electronics. With the exception of the propulsion pods, each system can be removed and replaced without the use of hand tools.

The height of the antennas for communication and sensing is an important design parameter dictating form factor. Early tests with prototypes indicated that the antennas for the GPS, GSM, and 802.15.4 radios all needed to be at least 2.5 cm off the water surface to guarantee a consistent signal.

Another parameter dictating form factor and overall dimensions was mission life. The external diameter of the main hull is fixed by the pre-fabricated housing chosen for the upper hull. However, the overall length of the vehicle into the water could be varied to accommodate more or less battery. The final vehicle length was chosen to accommodate a battery capable of 72 h of mission life (see section 'Electronics' for details) while not violating the man-portability functional requirement.

Finally, it was imperative that the mass be distributed so that the vehicle be hydrostatically stable in the desired orientation. Therefore, the battery was located low in the vehicle to ensure that the center of mass was below the center of buoyancy. The motor pods were also located as close to the center of mass as possible in order to minimize any unnecessary moments acting on the vehicle during steady-state operation.

Sensing

The fundamental sensing mission of the vehicle is to measure the river velocity and to make measurements of water quality factors. Because velocity is not uniform across the water column, hydrodynamic models are needed to infer the velocity deep in the water, hence the necessity of the backend computing infrastructure discussed previously.

The water quality sensor currently used is the Omega CDE222 temperature/electroconductivity sensor. An estimate of the salinity of the water can be made from these two quantities. The Omega CDE222 is normally a hand-held laboratory sensor; it is inexpensive, and its form factor is convenient for integrating directly into the drifter, making it a good choice for a representative water quality sensor.

The most convenient way to estimate position and velocity in outdoor environments at reasonable accuracies is a civilian GPS unit. Factors to consider when selecting an OEM GPS unit include power consumption, form factor, accuracy, and ease of integration. The Magellan AC-12 GPS unit is slightly larger than other available units, but has higher accuracy; 1.0 m circular error probable (CEP) as opposed to 2.5 m CEP, which is the more usual accuracy of low-cost, commercial grade OEM GPS units. This GPS unit also provides an estimate of the velocity of the drifter. This is important both for the passive sensing function of the drifter as well as for control during active propulsion. Because of the non-trivial interaction between the thrust generated by the propellers, the rotational and linear drag from the surrounding water, and the unknown velocity of the surrounding water, it would be very difficult to estimate the velocity of the drifter based on the control input to the propellers. It is far easier to directly estimate the velocity of the device using the GPS module.

Estimating the vehicle heading is very important for any guidance or motion control operations. An estimate of heading can be made from GPS readings alone, but at the low speeds at which the vehicle moves, these estimates would be inaccurate to the point of inefficacy. A separate sensor, the Honeywell HMC6532, was chosen to provide heading information. The HMC6532 is an integrated circuit package containing two magnetometers and logic circuitry to translate those readings into a heading measurement relative to magnetic north. It provides roughly

2° accuracy at 20 Hz, which is appropriate for the heading control tasks faced by the vehicle.

Vehicles which have been modified for use with the Office of Naval Research also include a Hummingbird single-beam depth finder for bathymetry mapping.

Actuation

The objective of adding propulsion capability to a Lagrangian sensor is to enable it to stay off the banks and clear of obstructions in shallow water. In the case of adaptive sampling, it also enables the drifters to position themselves near features of the water which the user might want to monitor. Initial experiments with a fleet of 10 passive sensors in the Sacramento-San Joaquin Delta indicated that sensors got stuck after approximately one hour if left unattended. Therefore, the propulsion system was designed to re-orient the vehicle and enable it to perform brief course corrections to keep clear of river boundaries. However, given that the vehicle must present a large cross-sectional area to flow, it is not expected to achieve high velocities. A design speed target of 0.3 m/s was set to enable cross-stream movement, but not upstream movement or station keeping.

Initial actuated prototypes featured a single propeller with a gear driven rotary pod to re-orient the propulsive force as shown in Figure 8. However, the gear train occupied excessive space inside the vehicle and it was determined that the man-portability functional requirement would have been violated for this design approach to work. Also with single motor actuation, stability of the controller became an issue quickly.

Therefore the vehicle was redesigned with split motor control. In this configuration, the vehicle has two motor/propeller modules, one on either side of the vehicle. This allows two degrees of freedom for independent control of orientation and forward velocity. To achieve forward motion, the onboard computer compares the desired GPS waypoint to the current location of the vehicle. The computer calculates the bearing that the vehicle must maintain to reach the GPS waypoint, and the vehicle uses the electronic compass to drive itself toward the desired waypoint along the required heading. A feedback controller is used to control the two independent motors in order to maintain desired heading and speed, given feedback from the compass and GPS.

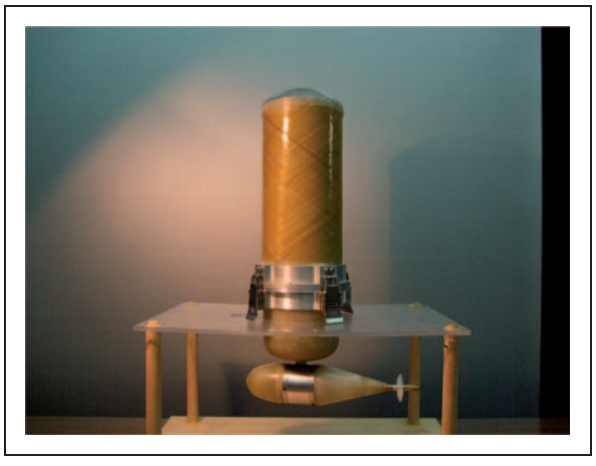

Figure 8. Single propeller design candidate which did not meet portability functional requirement and presented stability issues.

Angular velocity characterization. In order to investigate the suitability of different heading controllers for the sensor, a mathematical model of the vehicle's response to motor inputs was desired. A pre-production prototype was designed with split motor control and optical encoders on each motor shaft so that the angular response of the vehicle could be mapped to the difference in revolutions per minute (RPM) between the two motors. To generate data for the model, a high-speed camera was used to track the vehicle's angular displacement as a function of time to known motor inputs.

The model is based on the law of dynamics for angular motion, i.e. that the net torque on an object equals its moment of inertia multiplied by its angular acceleration. In the equation below, θ represents the angular displacement of the vehicle, I is the moment of inertia, and τ is the torque.

$$\tau = I \cdot \ddot{\theta} \tag{1}$$

A net torque will act on the vehicle when there is a difference in RPM between the two motors, ΔRPM. There will also be a drag torque, which is assumed to be directly proportional to the angular velocity. Thus, the equation above becomes an ordinary differential equation in which ΔRPM acts as a control:

$$c_1 \Delta\text{RPM} - c_2\dot{\theta} = I \cdot \ddot{\theta} \tag{2}$$

In the equation above, c_1 and c_2 represent unknown constants to be determined by a polynomial approximation of the high-speed camera data shown in Figure 9.

The vehicle response was modeled in Simulink. The block diagram of the plant is reproduced in Figure 10.

Heading controller comparison. The creation of an accurate vehicle model enabled an investigation into the suitability of multiple heading controllers for the sensor. The function of the heading controller is to apply power to the motors in order to orient the sensor along a given trajectory in a stable and time-efficient manner. Three types of controller were investigated: proportional (P), proportional-integral-derivative (PID), and model-based.

The simplest of these is a proportional controller. In this scheme, the magnitude of the control input is

directly proportional to difference between the desired state and the current state. In this context, the desired state is the desired heading of the sensor and the current state is its current heading. The blue line in Figure 11 shows a simulation of a sensor starting at zero radians and turning to $\pi/2$ radians under proportional control. The simulation shows that the sensor overshoots the desired heading and oscillates before settling to the desired heading. This is expected because the form factor of the vehicle enables it to rotate rapidly. Therefore, the second motor is not capable of countering the sizable angular momentum of the vehicle as it approaches the desired heading, resulting in osculations. The magnitude of the overshoot can be minimized by reducing the proportional control gain. However, this results in the sensor taking excessive time to reach the desired heading.

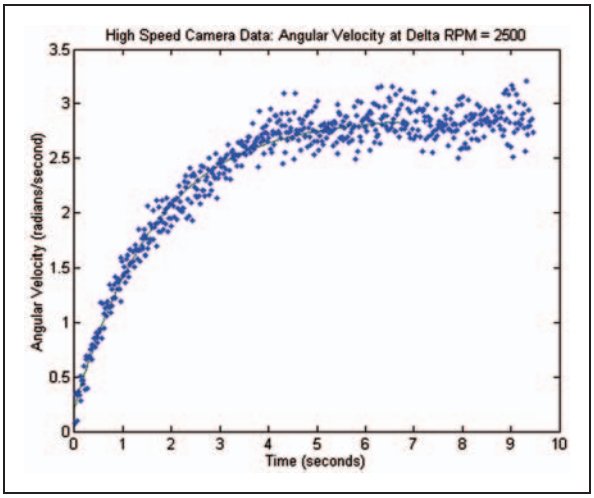

Figure 9. Angular velocity data for the vehicle model.
RPM: revolution per minute.

Thus, it was deemed that proportional control would not be effective for this system.

In order to minimize the controller overshoot, a PID controller was simulated. This control scheme adds terms for the integral and derivative to the calculation of the control effort. The derivative term prevents the overshoot by reducing the control effort if the sensor is rapidly approaching the desired heading. The integral term adds control effort as a function of time if the sensor dwells far from the desired heading. The relative control gains can be tuned heuristically or with automated methods. The black line in Figure 11 shows the result a PID controller applied to the system. It can be seen that the overshoot and oscillation is reduced in this scheme.

Finally, a model-based controller was simulated for the vehicle. In this scheme, the data from the vehicle model is uploaded to the vehicle's controller. This design has the advantage that it can more accurately predict when the vehicle is approaching the desired heading, minimizing the chances of overshoot. This controller worked well on prototypes and successfully minimized overshoot and settling time, as seen in the red line of Figure 11. However, the use of this controller requires that shaft encoders be installed on every production vehicle. It was determined that the added cost and complexity of this approach was not worth the marginal improvement in settling time compared to the PID controllers. Thus, the production fleet uses PID controllers.

Forward velocity characterization and validation. Once the vehicle size requirements and control were determined, motors and propellers had to be sized to meet the target forward velocity of 0.3 m/s. The vehicle drag coefficient estimate, C_d for forward motion is $C_d = 0.8$, based on calculations for an ideal

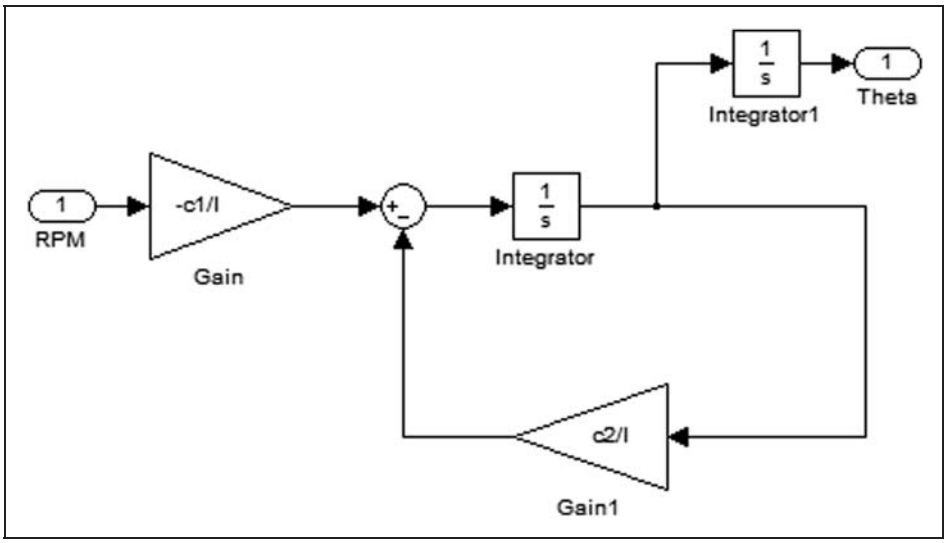

Figure 10. Vehicle plant for control simulation, designed in Simulink.
RPM: revolution per minute. 'RPM' represents ΔRPM, 'Theta' represents the angular displacement of the vehicle, and c_1 and c_2 are the constants defined previously.

finite cylinder.[18] Vehicle cross-sectional area, A was determined by CAD program to be $0.032\,m^2$. These numbers are used to estimate the steady-state speed, v of the vehicle with respect to the water as it travels in a straight line with the sum of the two propeller forces operating at F_{prop}. Equating drag force to propulsive force (with water density, ρ)

$$F_{drag} = \frac{1}{2}\rho C_d A v^2 = F_{prop} \tag{3}$$

Solving for F_{prop} in this equation with $v = 0.3\,m/s$, the desired propulsion force is 1.15 N or 0.58 N per motor. A test setup was developed consisting of a force load cell attached to a motor/propeller pod (Figure 12). The motor was driven by a speed controller at a range of speeds at 7.4 V and the output force was logged as function of input power. A number of motor/propeller combinations were explored. The chosen combination produced the most force per unit input power near the 0.58 N target (Figure 13).

The actual speed of the vehicle was estimated during tests in an outdoor tank at the UC Davis Bodega Bay Marine Laboratory. By driving back and forth in the still water of the tank, while receiving GPS signals, the speed of the vehicle can be estimated. Two techniques were used: first, the GPS velocity signal itself was averaged over a run across the pool, providing an estimate of 0.264 m/s with a standard deviation of 0.036 m/s. An alternate method is to take a finite difference of the GPS positions, spaced 6 s apart: this method results in an estimate of 0.242 m/s with a standard deviation of 0.033 m/s. It is expected that the finite difference estimate would be lower, because the drifter does not travel in a perfectly straight line. Figure 14 shows the time series of the speed estimates by the two methods during a run across the pool, and Figure 15 shows the GPS positions gathered during the run.

Depth controller. Many interesting features of hydrological systems exist under the surface of the water. Therefore, it is desirable that the sensor be able to control its motion along the water column to take measurements at known depths.

During the design process, the authors investigated the possibility of adding this capability within the requirements outlined in the Ishikawa diagram.

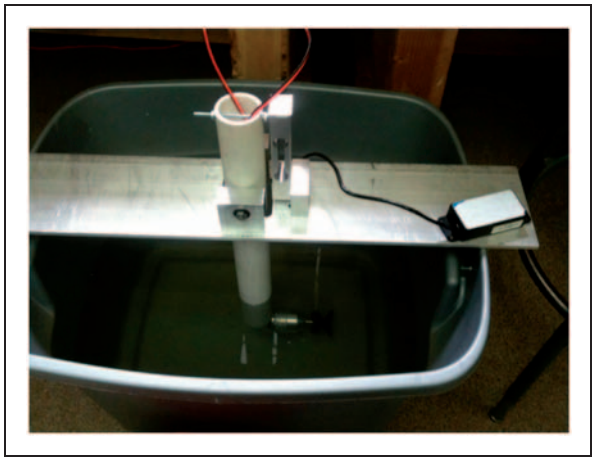

Figure 12. Motor force test platform: submerged motor unit is attached to an extended arm which pivots against a force transducer. Power is applied to the motor at a range of values and output force is recorded in Matlab.

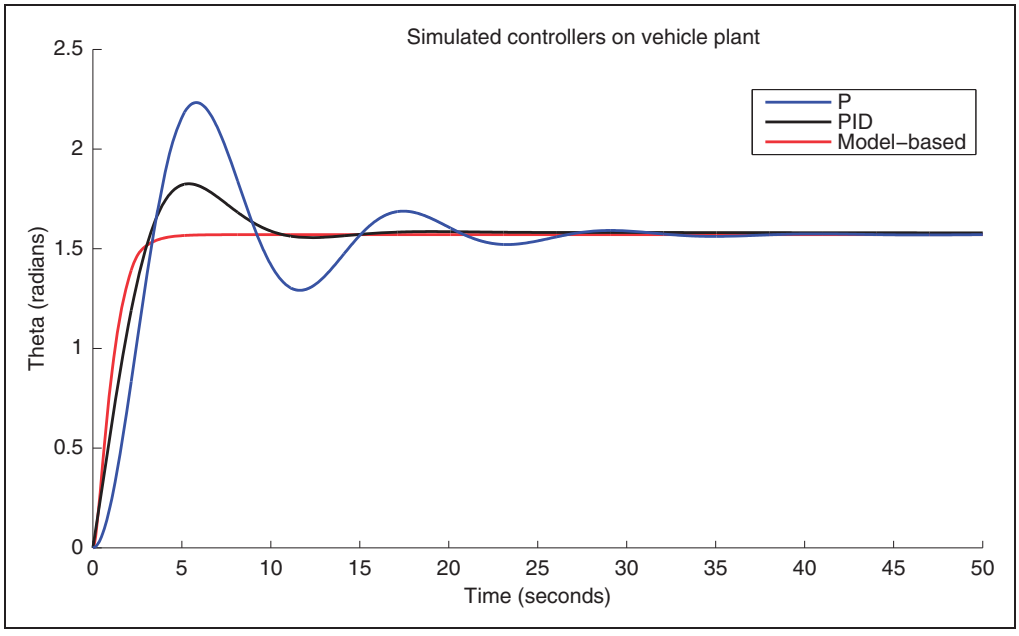

Figure 11. Simulink simulation of the effect of three proposed controllers on the vehicle plant.

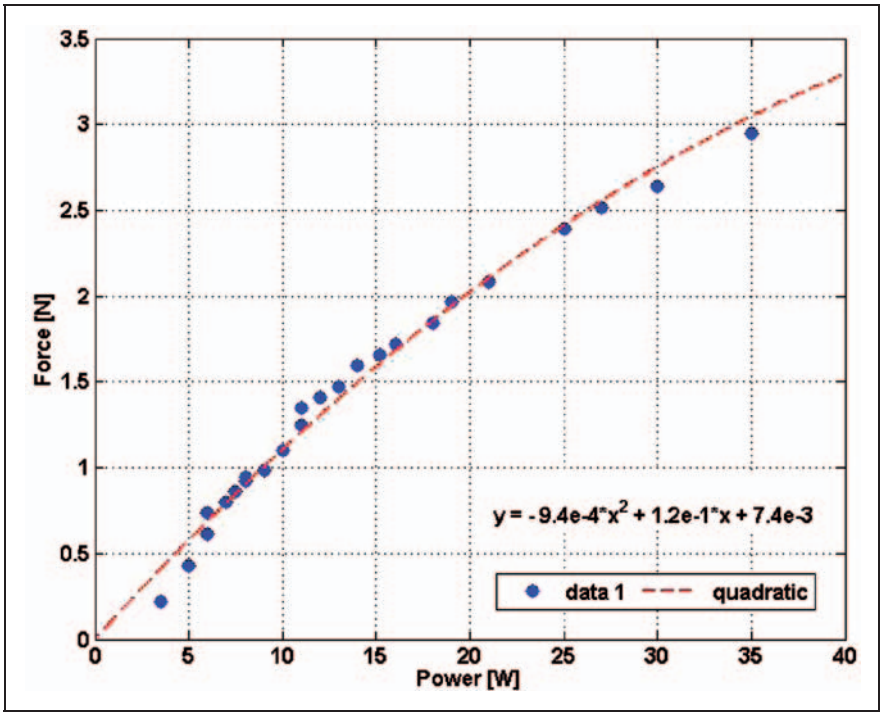

Figure 13. Output force as a function of input power for chosen motor/propeller.

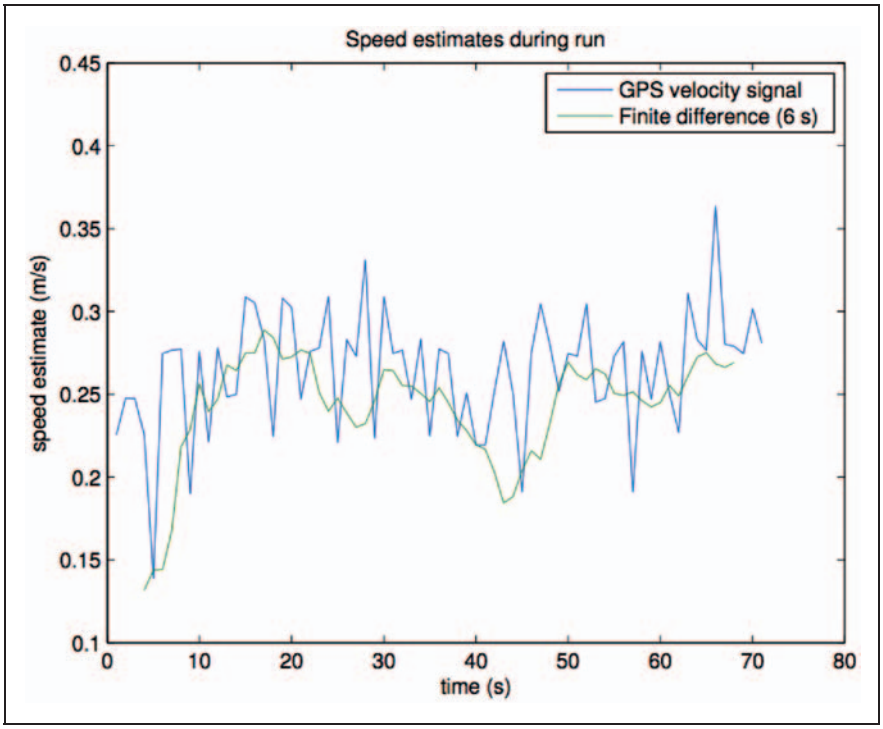

Figure 14. Vehicle velocity inferred from GPS signal.

A prototype sensor containing an adjustable ballast system was created. Ballast is added by drawing surrounding water into the vehicle through silicone tubes connected to a gear pump, as shown in Figure 16. The water is contained in a sealed reservoir in the upper hull of the vehicle.

A pressure sensor embedded in the lower PVC mounting plate is used to determine depth of the vehicle below the water surface, as shown in Figure 17. A proportional controller uses feedback from the pressure sensor to add and remove water from the ballast reservoir to adjust the sensor depth.

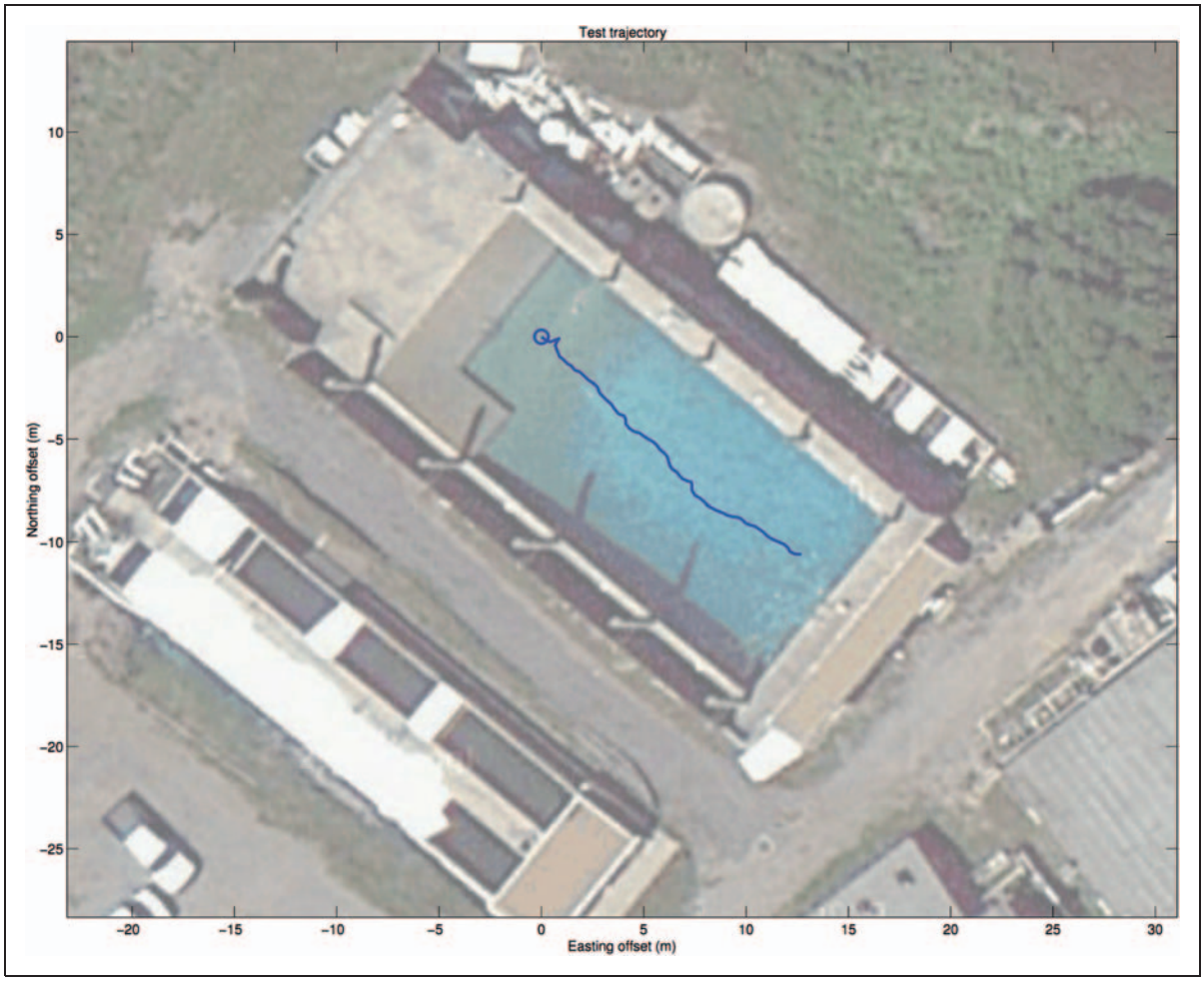

Figure 15. GPS trajectory from vehicle during velocity test.

Figure 16. Prototype sensor with buoyancy control.

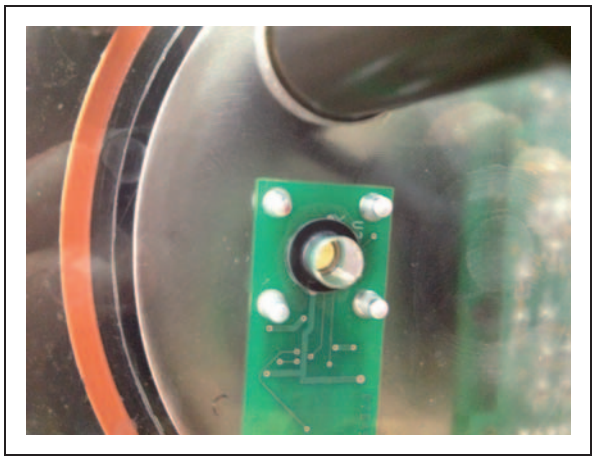

Figure 17. View of bottom PVC mounting plate with embedded pressure sensor.

Laboratory experiments in closed tanks revealed that this was a viable method of controlling depth. The sensors were able to perform multiple controlled dives to 5 m depth. However, integrating buoyancy into the final operational system presented non-trivial challenges.

First, the sensors lose GPS, GSM, and 802.15.4 connectivity when submerged. This presents two challenges: the sensors position is no longer known, and it is no longer able to communicate in the event of a failure. The first challenge could be addressed with a nine-degree of freedom inertial measurement unit. These units use filtered data from 3-axis accelerometers, gyroscopes, and magnetometers to estimate vehicle position from a known starting point; however, these are expensive and would require additional computational complexity. The communication challenge could be solved by creating a separate pod for communication equipment that stays on the surface of the water while the main hull is submerged. However, this would complicate the vehicle design and impinge upon the man-portability requirement outlined in the Ishikawa process.

Second, the failure modes of the system as designed can result in complete loss of the vehicle. If any component of the buoyancy system fails, it will begin to flood the vehicle. This would damage the electronics and likely result in the vehicle becoming completely submerged before a field team could retrieve it. This could be mitigated by adding a leak sensor that would automatically trigger the pump to empty the reservoir at maximum rate. However, if the pump jammed or a tube became obstructed this safety mechanism would be rendered useless. Therefore, though the current production vehicles can be modified for buoyancy control, this capability is not used in field operations.

Construction

As shown in the Ishikawa diagram, there are a number of functional requirements for the hull construction of the sensor. The most important parameters require that it be weatherproof and waterproof. This requires that the material maintain its tolerances underwater within a wide range of temperatures. It is also important that the design be scalable: that production can be rapidly increased after the first prototypes were produced.

Therefore, a high performance plastic, Acetal homopolymer (Delrin®) was chosen for the main hull construction. It is well suited to computer numerical control machining which allows scalability in manufacturing. It is also a material that can be injection molded at larger production quantities. Finally, it only absorbs 0.2% of its volume in water during 24-h submersion and has an operating temperature range of $-29\,^{\circ}C$ to $89\,^{\circ}C$.

Electronics

Computation

The vehicles were designed to be used as a research platform for investigating implementations of distributed robotics, multivehicle control, environmental sensing, and data assimilation. The computational requirements for controlling the vehicle and fulfilling mission goals therefore vary widely between scenarios. The computational hardware was therefore chosen to provide flexibility.

An embedded microprocessor system supporting the Linux operating system offered an efficient development process. Multitasking, file systems, databases, inter-process communications, and advanced memory management are examples of some of the useful features of a Linux operating system in this context.

One disadvantage of high-level systems such as a Linux-based embedded computer is that real-time control can be difficult to implement. This is because guaranteed timing of control tasks (which is essential for real-time control) is difficult to achieve in a general purpose operating system. A common solution, and one adopted here, is to split the control functionality between the high-level, non-real-time microprocessor and a low-level, real-time microcontroller to handle fast, time-critical control tasks.

Our selected embedded microprocessor is the Gumstix Overo Water, a single-board computer using the Texas Instruments OMAP 3530 Applications Processor running at 720 MHz, 512 MB of RAM, and a 2 GB MicroSD card for storage.[19,20] The Overo comes installed with mainline Linux 2.6.34 using the OpenEmbedded distribution and toolchain.[21] Earlier generations of Gumstix products featured a Gumstix microprocessor combined with an Atmel ATMEGA128 microcontroller for low-level tasks such as motor control.[22] Using this architecture as inspiration led to the selection of the Atmel XMEGA128[23] (a next-generation version of the ATMEGA) for the motor control and other low-level control tasks.

Power

Rechargeable electrochemical batteries are the cheapest and most convenient way to store the electrical energy needed for the onboard electronics and motors. The power budget for the electrical systems is shown in Table 1. The energy storage requirement is set by the power budget and mission time; the major remaining choice for the battery system is the battery chemistry, which will determine the mass, volume, and material cost of the battery that can store the required power. A summary of battery chemistries and their energy densities is shown in Table 2. Lithium ion and lithium polymer batteries are the only ones that are compatible with the mass and volume constraints of the hull (as discussed in section 'Form factor').

The electronic components and the motors require different input voltages. Although it would be easy to incorporate a voltage regulating circuit to lower the voltage for the electronics, allowing all systems to share a common battery, there are reasons why it

Table 1. Component power requirements.

Component	Voltage (V)	Current (A)	Duty cycle (%)	Power (W)
Overo	3.7	0.3	50	0.51
G24	3.7	0.2	5	0.04
XBee-PRO ZB	3.3	0.3	5	0.04
Motors	7.4	2.4	10	1.8

Table 2. Representative battery capacities for various chemistries.

Chemistry/format Example	Specific energy (kJ/kg)	Energy density (kJ/L)
Lithium ion Panasonic NCR18650 (ref.[24])	840	2100
Lithium polymer Sanyo UPF673791 (ref.[25])	760	1800
Nickel-metal hydride Panasonic HHR110AAO (ref.[26])	200	620
Lead-acid Panasonic LC-P0612P (ref.[27])	130	370

makes sense to keep the motor power separate from the electronics power. First, the inrush current when motors start can cause a voltage slump which could cause drop-outs in the electronics power; second, brushed DC motors can generate noise on the power lines that could adversely affect the electronics; and third, if the motors are run long enough to exhaust the battery, and the electronics are on the same battery, the vehicle will no longer be able to gather data or transmit its location. The first and second problems could be mitigated by careful design of the voltage regulator circuitry, but it is easier to simply keep the two power sources separate.

Our selected design was a hexagonal pack of 19 cylindrical lithium ion cells, with five cells dedicated to the electronics (3.7 V, 170 kJ, allowing 80 h of electronics operation) and 14 cells dedicated to the motors (7.4 V, 480 kJ, allowing 74 h of operation at the 10% duty cycle), see Table 1 for component power requirements.

Communications

There are three primary reasons to communicate with a drifting sensor in the field:

1. to discover the local water conditions for real-time sensing applications;
2. to track the sensor's position for retrieval, or to query its health and operational status (battery energy remaining, etc.);
3. to share data between vehicles for multi-vehicle control applications or with the command center for remote actuation of the drifter.

These goals have different requirements for transmission range, bandwidth, and latency. Goals (1) and (2) above have very low bandwidth requirements; 0.01–0.1 kB/s, with up to 30 s latency, would be acceptable. However, these transmissions will need to be sent over distances of kilometers or greater. By contrast, goal (3) requires more bandwidth and lower latency; 2 kB/s with < 1 s latency. For multi-vehicle control applications the vehicles can be assumed to be relatively close: 100 m is a reasonable range. These diverse requirements can be best addressed with two separate communication networks.

The range requirements of the long-range communication system pose a challenge in the estuarine environment. The vehicles themselves could be up to 10 km away from their origin. Islands, levees, trees, and buildings are all interfering obstacles. The best self-contained solution would be to erect a communication tower on-site to minimize the fading through these obstacles. Although truck-mounted portable tower solutions exist, there is a more convenient option: the civilian GSM network. Using a GSM module such as the Motorola G24,[28] the drifting sensor can use the general packet radio service (GPRS) of the GSM protocol suite[29] to open a TCP connection to any server on the Internet. The guaranteed minimum bandwidth of a GPRS connection is 9.6 kB/s, but the latency is not guaranteed. Empirical tests show that latency of 1–5 s is common.

Due to the larger latency, the GSM solution is inappropriate for multi-vehicle control applications. At shorter ranges, it is reasonable to expect a clean line-of-sight between the vehicles, and so a low-power point-to-point radio system is appropriate. The emerging IEEE 802.15.4 standard for low-power wireless networks[30] defines protocols for low-powered radios to form mesh networks and transfer small quantities of data (appropriate for sensor networks, automation, or other embedded applications) over the 2.4 GHz ISM frequency band. Some radios that conform to a subset of the IEEE 802.15.4 drafts are branded as *ZigBee* radios. The Digi XBee-PRO ZB is a ZigBee radio that allows short-range, line-of-sight, low-latency data communications between vehicles. One feature of the XBee-PRO ZB that distinguishes it from similar modules is the on-board power amplifier, which increases the transmit power to 50 mW, extending the transmission range of the system. The authors have observed connectivity at distances of up to 1 km in river environments when using these modules.

Case studies

The *Floating Sensor Network* team tested the various capabilities of the system with completed projects involving the US Army Corps of Engineers, the Office of Naval Research, and the California Bay-Delta Authority. The following sections describe how these case studies were used to test the functional

requirements of the system detailed in sections 'Vehicle design' and 'Electronics'.

US Army Corps of Engineers

One application envisioned for the *Floating Sensor Network* is responding to levee failures. Using the real-time web interface described previously, it would be easy to pinpoint the location of a levee breach and track the movement of water out of the system. It would also be useful for characterizing the change in salinity, temperature, and other important parameters after the breach has occurred.

To test this capability, the team was invited to participate in the 2009 Rapid Repair of Levee Breaches Demonstration in Stillwater, Oklahoma. The test was operated by the Department of Homeland Security and the US Army Corps of Engineers. A test levee was built at the Federal Agriculture Department's Hydrologic Engineering Research Unit shown in Figure 18.

The channel behind the levee was filled and the levee was breached, releasing 125 ft^3 of water every second. The sensors were deployed upstream and allowed to pass through the breach (Figure 19).

Despite a brief loss of GPS signal while the vehicle was submerged in the breach, the experiment demonstrated the robustness of the system for use in real-world environments and validated the design parameter dictating antenna height.

In addition to testing the robustness of the sensor design, this test offered an opportunity to test the data assimilation capabilities of the backend system. This experiment and the extended Kalman filter (EKF) analysis was first described by Tinka and Rafiee.[13] For the experiment, drifters were deployed into the supply canal upstream of the levee breach, shown in Figure 20. The upstream boundary condition was the supply canal flow control, set to 1.42 m^3/s; the downstream boundary condition was a gate that could be raised or lowered to restrict the flow out of the experimental region. Drifters were released at approximately 30s intervals near the upstream boundary, shown as Point A in Figure 20. After travelling through the canal for approximately 400s, they were individually retrieved near Point B of Figure 20. Point C of Figure 20 marks the location of the downstream control gate.

Figure 18. Test levee under construction.

Figure 19. Floating sensor about to pass through the breach.

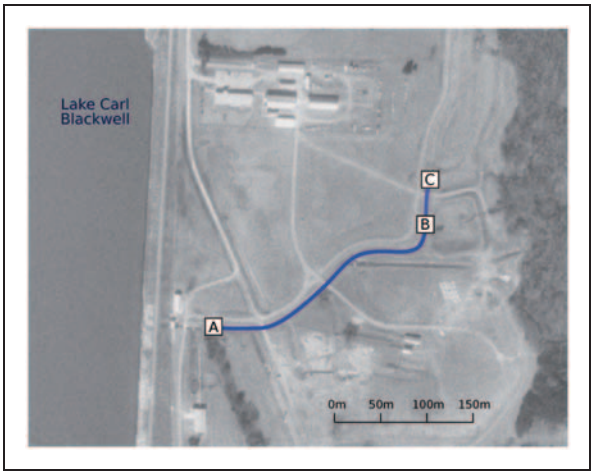

Figure 20. Annotated satellite image of supply canal.

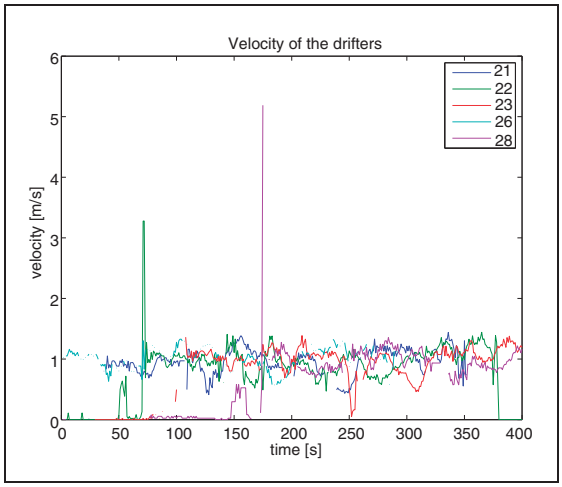

Figure 21. Measured sensor velocity during canal deployment.[13]

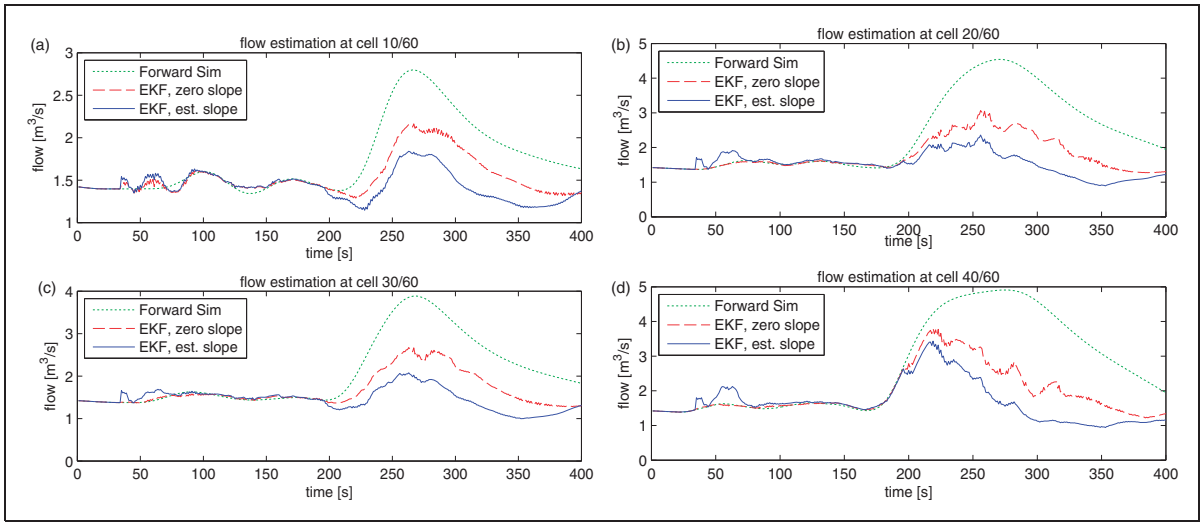

Figure 22. Estimated flow in discretized "cells" of the canal.[13]

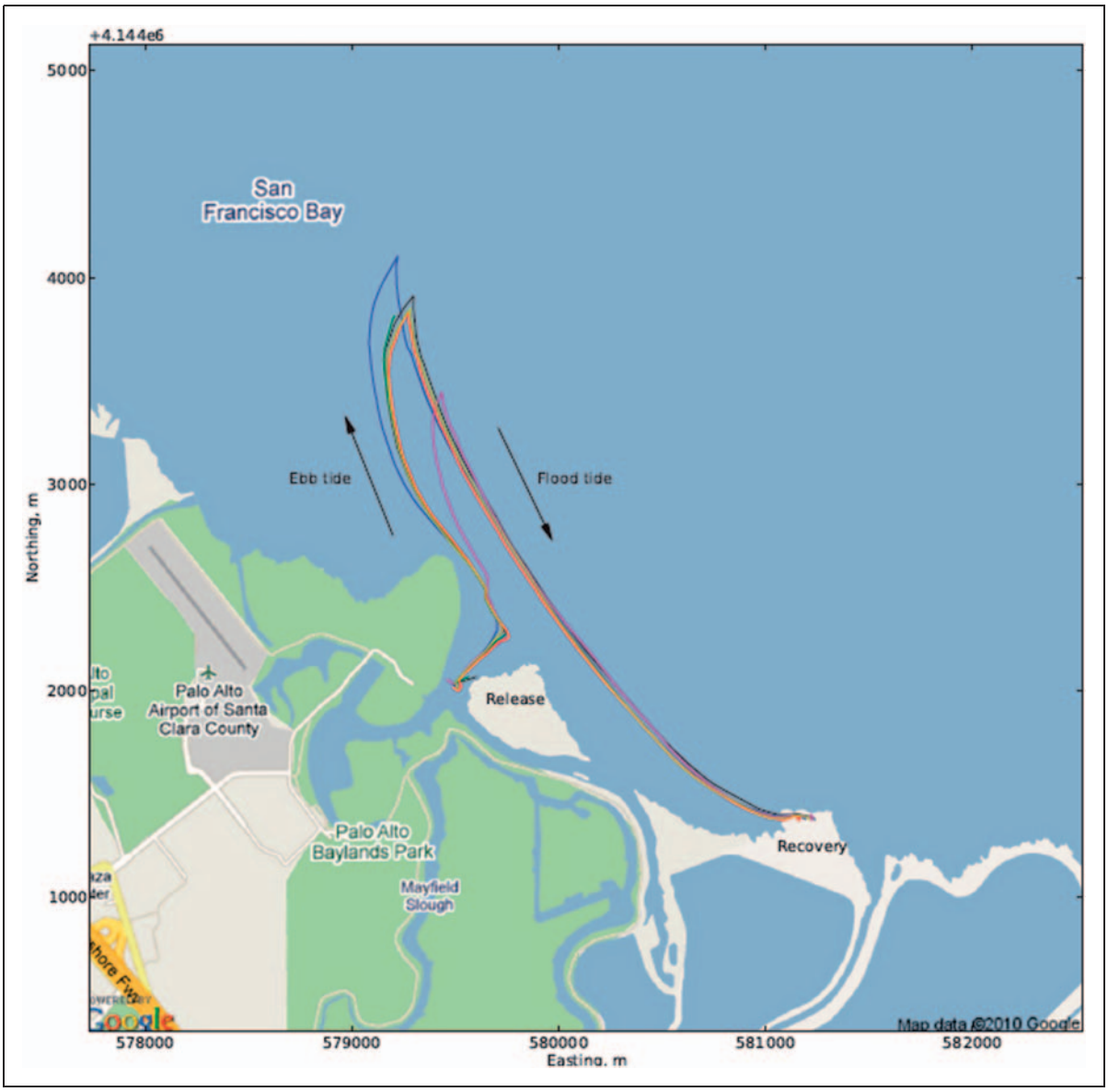

Figure 23. GPS traces from floating sensors during 24-h San Francisco Bay experiment.

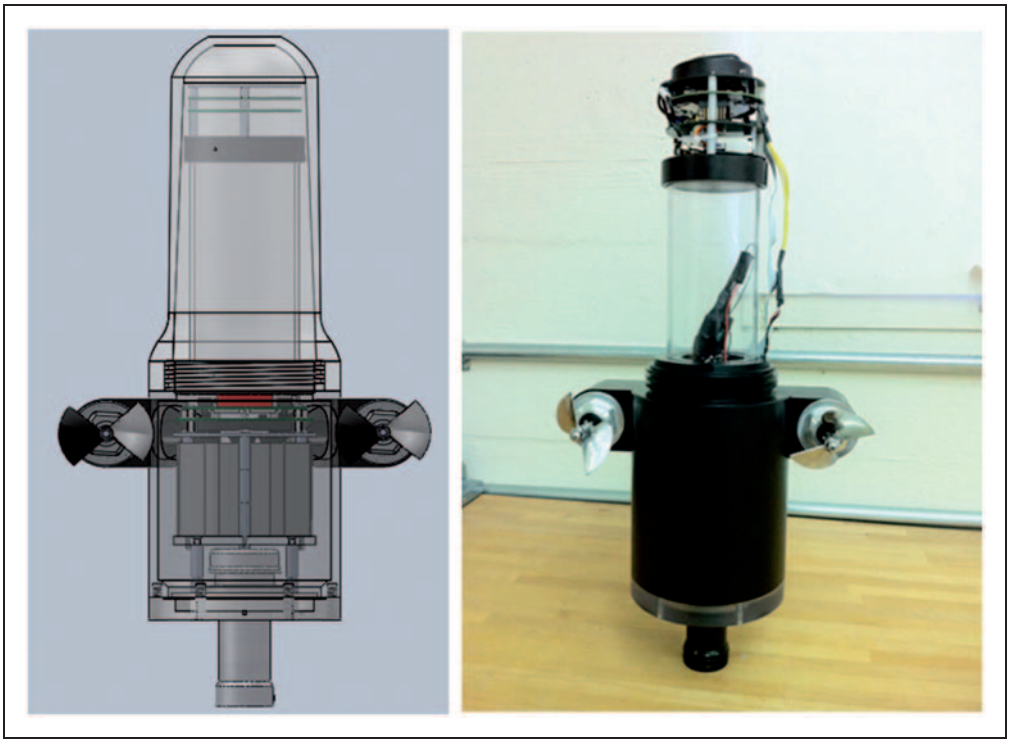

Figure 24. Floating sensor modified for single-beam depth finder.

A total of 20 runs were performed, and divided into five cycles of four runs each. Each run in the cycle had a different operation of the downstream control gate. During the first run, the gate remained open for the entire run. During the second run, the gate was closed as soon as the sixth drifter was released. During the third run, the gate remained closed. Finally, during the fourth run the gate was opened as soon as the final drifter was released. The cycle was then repeated.

The velocities of the sensors in one run are shown in Figure 21. The spikes in the velocity signal correspond to the sensor being thrown in the water. The velocity data from five sensors could then be assimilated with an EKF to estimate the flow in discretized 5 m regions of the channel. Figure 22 shows the flow estimation in discretized 'cells' using three techniques: forward simulation of the one-dimensional shallow water equation, and an EKF with and without estimating the bed slope.

The robustness of the sensor combined with the data assimilation system could be useful in the event of a levee failure in a region which supplies drinking water and is a fragile ecosystem for wildlife, such as the Sacramento-San Joaquin Delta. On 3 June, 2004, a levee breach occurred on the west levee of the Upper Jones Tract in the southern region of the Delta in San Joaquin County. It would be difficult to use the existing static infrastructure to track changes near the breach given that no infrastructure existed in the region prior to flooding. The floating sensors could be immediately deployed by small boat teams in the affected region and would be able to upload data in real time.

California Bay-Delta Authority

A number of experiments have been performed with the *Floating Sensor Network* to support research in the Sacramento-San Joaquin Delta region performed on behalf of the California Bay-Delta Authority. The sensors have been used to track temperature changes near the Jones Tract failure and the implications for the delta smelt fish in the region. Other researchers have used the sensors to study the effect of submerged vegetation on water flow.

The sensors have also been used in the San Francisco Bay to study the exchange of water between the Bay and the rivers that feed into it. In May 2010, the sensors were deployed near the Mayfield Slough in the South San Francisco Bay. They were tracked over a full tidal cycle to determine if particles which get pulled into the Bay during the ebb tide return during the flood tide, as shown in Figure 23. Unfortunately, high winds resulted in the data not matching the exact expectations of hydrodynamicists involved in the experiment, but the operation confirmed the ability of the system to operate unattended overnight and be retrieved. It also validated the design parameters governing battery life and mission time.

The experiment also reinforced our confidence in the design parameters indicating that multiple communication methods are necessary. During the

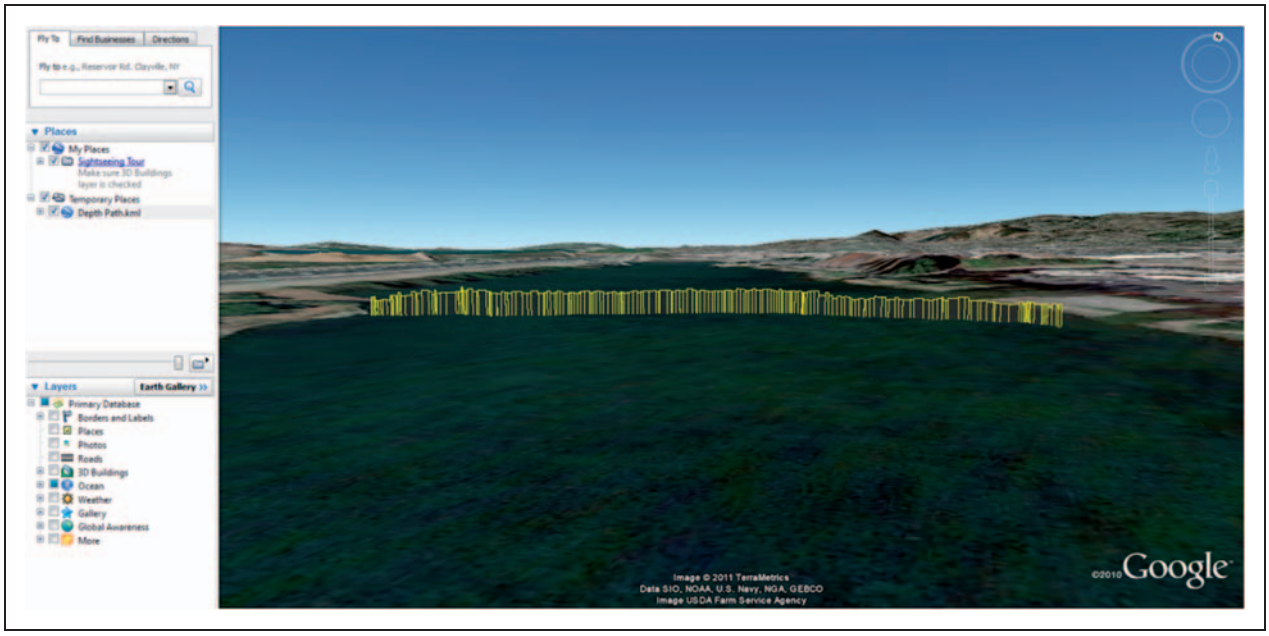

Figure 25. Automated depth survey from sensor path shown in Google Earth.

middle of the night, the GSM signal unexpectedly failed (likely due to limited coverage in the center of the Bay). Without the capacity to communicate over the 802.15.4 radios, the vehicles would have been unrecoverable.

Office of Naval Research

The *Floating Sensor Network* was also explored as a platform for autonomous depth mapping of rivers for the Office of Naval Research. As part of phase one SIBR with SSCI, Inc., the team redesigned the sensors to be able to carry single-beam depth finders (Figure 24).

SSCI developed a number of strategies in which the vehicles could leverage inter-vehicle communications to coordinate while operating in unstructured environments to upload depth maps in real time. Tests were done at the aquatic park near UC Berkeley and the data were uploaded to Google Earth (Figure 25).

This application underscored the importance of design modularity. The sensor network was not designed with this application in mind but was able to accommodate the new application with limited changes to the system design thanks to the modular PVC sensor mounting plate and flexible electronics design. It also validated the computation design parameters such as the need to have a powerful processor for coordinated control tasks with a separate low level controller for real-time control.

Conclusion

This article has described how the Ishikawa design methodology can be applied to developing a new network of robotic sensors for autonomous water management in near-shore environments. Specifically, it describes how the design parameters for the system evolved from a more general set of functional requirements which are interconnected through a cause and effect diagram. As a result of this design and prototyping process, a number of general conclusions are reached for the system.

First, when designing a sensing solution for multiple end users, it is important to have a modular sensor mounting system. The case studies confirmed that there are a number of applications for the sensor network ranging from bathymetry mapping in remote environments to salinity tracking for environmental monitoring purposes. If the system is to be broadly applicable, it must be able to accommodate a diverse set of applications with minimal changes to the core system design.

Second, the longer field tests have underscored the importance of redundant communication devices for retrieval. When GSM connectivity was lost during the 24-h experiment in the San Francisco Bay, retrieval would have been impossible without having the ZigBee radios as a backup.

Third, the case studies have confirmed the need for actuation for Lagrangian sensors in near-shore environments. Field experiments which featured passive and active sensors deployed at the same time in the same location showed that passive sensors were only effective for 10 min before becoming entangled on shore whereas the active sensors operated for over an hour without becoming entangled.

Fourth, the 72-h mission target seems to be sufficient for near-shore environments. Due to the small experimental domains of riverine networks, the sensors usually leave the experimental region in

under 10 h. The 24-h test in the San Francisco Bay is the longest mission requested thus far.

Finally, the authors believe that the vehicle form factor presents a reasonable tradeoff between manportability, Lagrangian sensing, and active control capacity. Further design studies could consider a more formal approach to optimizing vehicle size, battery life, and actuation mechanisms.

Funding

This work was supported by funding from Scientific Systems Company, Inc. by subcontract 1516 from the Office of Naval Research, and by awards 0845076 and 0931348 from the National Science Foundation.

References

1. Swallow JC. A neutral-buoyancy float for measuring deep currents. *Deep Sea Res* 1955; 3(1): 74–81.
2. Gould WJ. From swallow floats to Argo–the development of neutrally buoyant floats. *Deep Sea Res Part II: Top Stud Oceanogr* 2005; 52(3–4): 529–543.
3. Clark DD. Overview of the Argos system. In: *Proceedings of OCEANS '89*, Seattle, Washington, USA, vol. 3, 1989, pp.934–939.
4. Davis RE. Drifter observations of coastal surface currents during CODE: the method and descriptive view. *J Geophys Res* 1985; 90(C3): 4741–4755.
5. Niiler PP, Davis RE and White HJ. Water-following characteristics of a mixed layer drifter. *Deep-Sea Res* 1987; 34(11): 1867–1881.
6. Oki T and Kanae S. Global hydrological cycles and world water resources. *Science* 2006; 313: 1068–1072.
7. Detweiller C, Vasilescu I and Rus D. An underwater sensor network with dual communications, sensing, and mobility. In: *OCEANS 2007-Europe*, Aberdeen, Scotland, New York: IEEE, 2007, pp.1–6.
8. Sujit PB, Sousa J and Pereira FL. UAV and AUVs coordination for ocean exploration. In: *OCEANS 2009-EUROPE*, IEEE, 2009, pp.1–7.
9. Han Y, de Callafon RA, Cortés J, et al. Dynamic modeling and pneumatic switching control of a submersible drogue. In: *7th International conference on informatics in control, automation and robotics*, Funchal, Madeira, Portugal, 2010, pp.89–97.
10. Bhatta P, Fiorelli E, Lekien F, et al. Coordination of an underwater glider fleet for adaptive ocean sampling. In: *Proceedings of international workshop on underwater robotics*, Genova, Italy, 2005.
11. Ryan J, Aonghusa N and Sweeney E. SmartBay, Ireland: design and planning for a cabled ocean observatory off the west coast of Ireland. In: *OCEANS 2007*, Vancouver, British Columbia, Canada, New York: IEEE, 2008, pp.1–4.
12. Floating Sensor Network project (2010) Available at: http://float.berkeley.edu (accessed 23 May 2012).
13. Tinka A, Bayen AM and Rafiee M. Floating sensor networks for river studies. *IEEE Syst J* 2012. Epub ahead of print. DOI:10.1109/JSYST.2012.2204914.
14. Tossavainen OP, Percelay J, Stacey M, et al. State estimation and modeling error approach for 2D shallow water equations and Lagrangian measurements. *Water Resources Res* 2011; 47(10). Epud ahead of print. DOI: 10.1029/2010WR009401.
15. Strub I, Percelay J, Tossavainen OP, et al. Comparison of two data assimilation algorithms for shallow water flows, I. *Netw Heterog Media* 2009; 4: 409–430.
16. Ishikawa K. Cause and effect diagram. In: *Proceedings of the international conference on quality control*, Tokyo, 1969, pp.607–610.
17. Wilson J and Wright P. Design of monocular head-mounted displays, with a case study on fire-fighting. *Proc IMechE, Part C: J Mechanical Engineering Science* 2007; 221(12): 1729–1743.
18. Zdravkovich MM, Brand VP, Mathew G, et al. Flow past short circular cylinders with two free ends. *J Fluid Mech* 1989; 203(1): 557–575.
19. Gumstix Overo Water COM. Portola Valley, California (2011) Available at: http://www.gumstix.com/store/product_info.php?products_id=228 (accessed 15 April 2012).
20. OMAP3530/25 Applications Processor. 2009.
21. Lauer M. Building Linux distributions with BitBake and OpenEmbedded. In: *Proceedings of the free and open source developers European meeting (FOSDEM 2005)*, Brussels, Belgium, 2005.
22. Gumstix Robostix. Portola Valley, California (2011) Available at: http://www.gumstix.com/store/product_info.php?products_id=139 (accessed 15 April 2012).
23. AVR XMEGA A3 Device Datasheet. San Jose, CA, 2010.
24. NCR18650 Datasheet. 2010.
25. UPF673791 Datasheet. 2011.
26. HHR110AAO Datasheet. 2004.
27. LC-P0612P Datasheet. 2000.
28. Motorola G24 Developers' Guide: Module Hardware Description. 2007. 6889192V27-G.
29. 3GPP TS 23.060 Version 10.4.0. Digital cellular telecommunications system (Phase 2+); universal mobile telecommunications system (UTMS); General Packet Radio Service (GPRS); Service description; stage 2'. 2011.
30. IEEE P802.15.4e/D0.01. Draft standard for information technology: telecommunications and information exchange between systems: local and metropolitan area networks: specific requirements: part 15.4: wireless Medium Access Control (MAC) and Physical Layer (PHY) specifications for Low-rate Wireless Personal Area Networks (WPANS) Amendment 1: add MAC enhancements for industrial applications and CWPAN, 2009.